Systematic dislocation analysis assessment by HAADF STEM imaging

L. Agudo Jácome[1], Ch. Somsen[1] and G. Eggeler[1]
1. Institut für Werkstoffe, Ruhr-Universität Bochum, D-44780, Bochum, Germany.

corresponding author: leonardo.agudo@rub.de
Keywords: dislocation analysis, HAADF, STEM, intermetallics, stereography

It is well known that transmission electron microscopy is a powerful method for dislocation analysis. This requires either the precise simulation of comparative dislocation images or the use of the invisibility criteria $\mathbf{g}\cdot\mathbf{b} = 0$ and $\mathbf{g}\cdot(\mathbf{u} \times \mathbf{b}) = 0$, where **g** is the reciprocal lattice vector, **u**, a vector along the dislocation line direction, and **b**, the burgers vector. In the latter case, at least two invisibility conditions $\mathbf{g_1}\cdot\mathbf{b} = 0$ and $\mathbf{g_2}\cdot\mathbf{b} = 0$ must be met in perfect two-beam conditions; usually a minimum of seven two beam conditions need to be considered in order to find these invisibility conditions and, once they are found, it is not easy to locate the dislocations because they are no longer visible. Additionally, the determination of **u** and of dislocation densities can be performed using 3D imaging techniques, like for example stereography [1]. Again, visualization of 3D images by stereographs is not straightforward, for it requires creating the illusion of a 3D image from two 2D micrographs. Moreover, it is often difficult to follow specific dislocation segments when dislocation densities are high or when other contrasts interfere with the image of the dislocation.

In this study, high angle annular dark-field (HAADF) imaging was carried out to analyze dislocations in the Ni-base single crystal superalloy LEK 94. A single crystalline rod was oriented in [001] direction by the Laue technique and then miniature creep samples were spark-eroded [2]. The [001]-oriented sample was crept at 1020°C and 200MPa until rupture (rupture time: 56.6h). TEM foils were extracted from gauge and head regions. Figure 1a shows a TEM bright-field image oriented in [010] direction obtained from a foil taken out of the head of the crept sample. In Figure 1b the corresponding STEM image obtained using HAADF contrast is presented. The dislocation segments are all clearly visible. Figure 2a shows a TEM bright-field image in two-beam contrast (**g** = [001]) obtained from the stressed region in the gauge length. In Figure 2b the same region is imaged with the HAADF detector but now in [010] direction. HAADF reveals dislocation segments that are invisible in Figure 2a marked with white arrows in Figure 2b. In γ-channels, where dislocations densities are high, the contrast is significantly enhanced. In addition, γ'-cutting processes by superdislocations can be clearly recognized. The bright line contrasts in Figures 1b and 2b document that dislocations effectively re-direct electrons from the primary beam towards the HAAD-detector by scatter/diffraction processes. HAADF dislocation imaging is a promising technique which we will use in further investigations.

1. A. Dlouhý and J. Pesicka, Czech Journal of Physics 40 (1990) p.539.
2. G. Mälzer et al., Metallurgical and Materials Transactions A 38A (2007) p.314
3. The research department IS^3/HTM is specially acknowledged for its financial support.

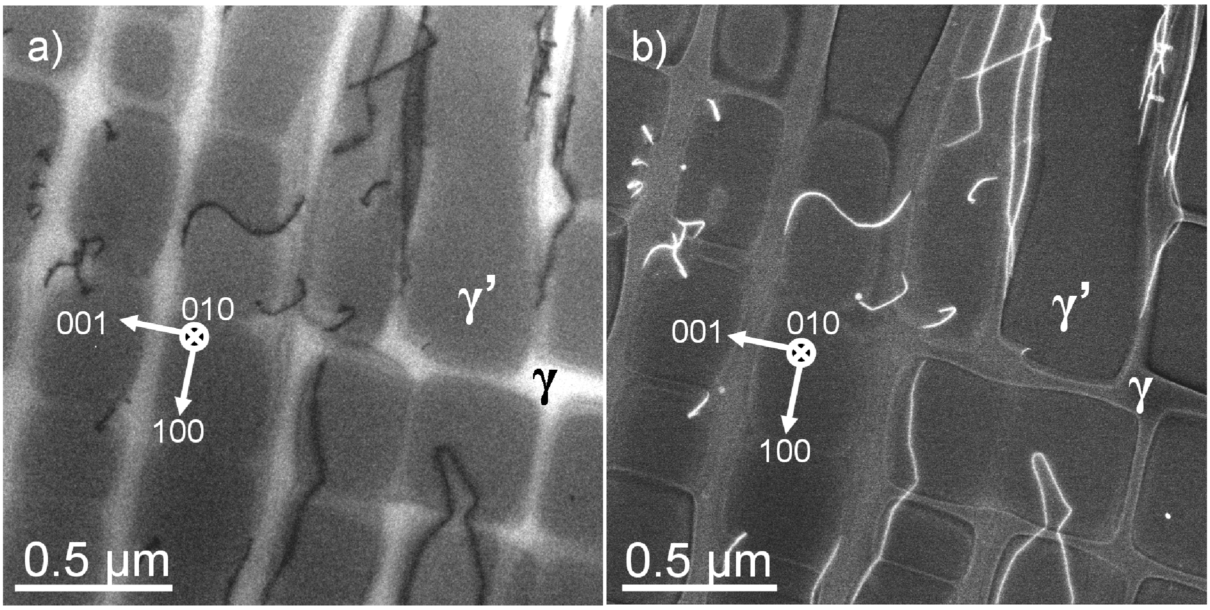

Figure 1. Single crystal superalloy LEK 94. Micrographs from the undeformed sample head after creep to rupture in [001] direction (1020°C, σ=200MPa, ε_r=26%). a) TEM bright-field image in [010] zone direction. b) HAADF-STEM image in [010] zone direction. Significant contrast improvement is observed in HAADF-STEM imaging.

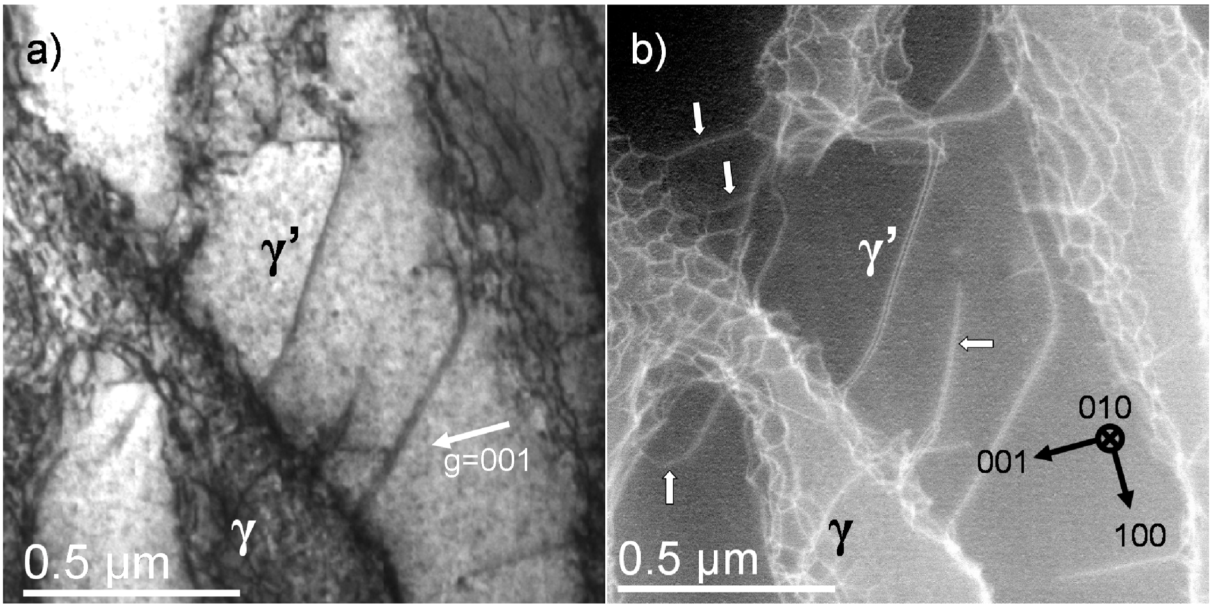

Figure 2. Single crystal superalloy LEK 94. Micrographs from crept region (1020°C, σ=200MPa, ε_r=26%). a) TEM bright-field image in two-beam case with **g** = [001]. b) HAADF-STEM image in [010] zone direction. HAADF-imaging reveals the features of the dislocation networks in the γ-channels and dislocation pairs cutting through γ' more clearly. White arrows in Figure 2b show dislocation segments which are invisible under the contrast conditions used in Figure 2a.

W. Grogger, F. Hofer, P. Pölt (Eds.): MC2009, Vol. 3: Materials Science,
DOI: 10.3217/978-3-85125-062-6-473 , © Verlag der TU Graz 2009